Mechanical characterization of orthotropic materials with speckle interferometry and numerical optimization

C. Barile, C. Casavola, G. Pappalettera, C. Pappalettere
Politecnico di Bari, Dipartimento di Ingegneria Meccanica e Gestionale, Viale Japigia 182, Bari, 70126, Italy
casavola@poliba.it

ABSTRACT. This paper describes the process of mechanical characterization of orthotropic materials. An hybrid approach based on the combination of phase-shifting electronic speckle pattern interferometry (PS-ESPI) and finite element analysis is utilized. Three-point-bending experimental tests are carried out. The difference between displacement values measured with ESPI and their counterpart predicted by FEM analysis is minimized in order to find the values of the unknown elastic constants.

INTRODUCTION

The displacement field of a specimen generally loaded and constrained is univocally defined if material properties are known. Obtaining the elastic constants from the measured displacement field is a reverse problem that can be solved by minimizing the difference between displacements measured experimentally and their equivalent computed by FEM analysis. This procedure allows obtaining mechanical properties of materials in all cases in which it results difficult and expensive to perform traditional mechanical tests. Non-contact optical techniques such as *Electronic Speckle Pattern Interferometry* (ESPI) [1,2] result appropriate for the measurements of displacement on a real component under working load: displacements can be accurately measured in real time and full field information can be obtained without altering specimen conditions. ESPI can measure displacement components u(x,y,z), v(x,y,z) and w(x,y,z) for each point (x,y,z) of the specimen surface. A system of fringes will appear on the specimen surface and each fringe represents the locus of an iso-displacement region. The frequency distribution of fringes can be used for recovering strain fields. In this study, three-point-bending tests are carried out on different materials and ESPI technique is used to capture the displacement field. The experimental procedure was chosen in order to avoid rigid body motion and prevent speckle pattern decorrelation. FE model is build by Ansys ® commercial code in order to reproduce the experimental set up (load and constraints of bending test). The difference between measured displacements and the computed ones is minimized and material properties can be evaluated. The aim of this work is to define the experimental set up and the optimization algorithm in order to obtain the mechanical properties of a new material obtained by means of selective laser melting process.

EXPERIMENTAL TESTS

Two types of metallic materials were studied: the first one was an isotropic and homogeneous titanium alloy; the second one was a mix of powder metallic realized by means of the Selective Laser Melting technique (SLM).
Titanium specimens were made of Ti6Al4V alloy and were subjected neither to thermal treatment either to mechanical process that could modify the material properties reported in Tab. 1. Titanium tests were planned in order to define the experimental set up and to validate the numerical model that could be used to study also new materials, as sintered components realized by means of non-conventional techniques.

	Young's Modulus [GPa]	Poisson's ratio
Titanium	110	0.32
Metal powders	207	0.3

Table 1: Titanium and metal powders mechanical characteristics

In SLM, parts are built by adding layers of metal powder through a focused laser beam that selectively fuses powdered material. This type of process modifies the initial mechanical characteristics of metal powders (see Table 1), which strongly depend on process parameters (i.e. laser energy, scanning strategy) and are hardly predictable. For this reason, the elastic constants of sintered materials are unknown and should be experimentally determined. Building SLM parts is rather expensive, so traditional mechanical tensile tests are generally executed on a limited number of specimens. The hybrid procedure proposed in this work should simplify the mechanical characterization of SLM part by using a finite element model, where all mechanical properties are unknown, and an optical measurement of displacement produced in a 3-point bending test. FEM and experimental displacements difference is then minimized by means of an optimization process.
Geometry of titanium specimen is 95.56 mm x 3.06 mm x 51.50 mm, whereas the sintered specimen is 127.5 mm x 2.79 mm x 35 mm. Both the specimens were placed on two supports at a distance of 90 mm. The beams were preloaded in order to minimize rigid body motions, which may cause speckle decorrelation. A thin coating layer was sprayed onto the specimen surface to improve contrast of speckle fringes. The loading apparatus is shown in Figure 1 together with a detail of the ESPI setup. A 2 kg loading cell DS 514QD was connected to the wedge in order to measure the applied load. Data were recorded by the Micro Measurements System 5000 acquisition system. The load was transferred by a micrometric translational stage, which pushes the loading wedge against the specimen. In order to ensure a correct application of the load, 4 strain gages were placed on the specimens' surface: 2 on the upper surface along the axis and far 10 mm from the edges, 2 on the lower surface in correspondence of the middle section and far 5 mm from the lateral edges. The real values obtain from the strain gages during the test, confirm that the load was uniformly distributed and was exactly applied in the middle section of the specimen.

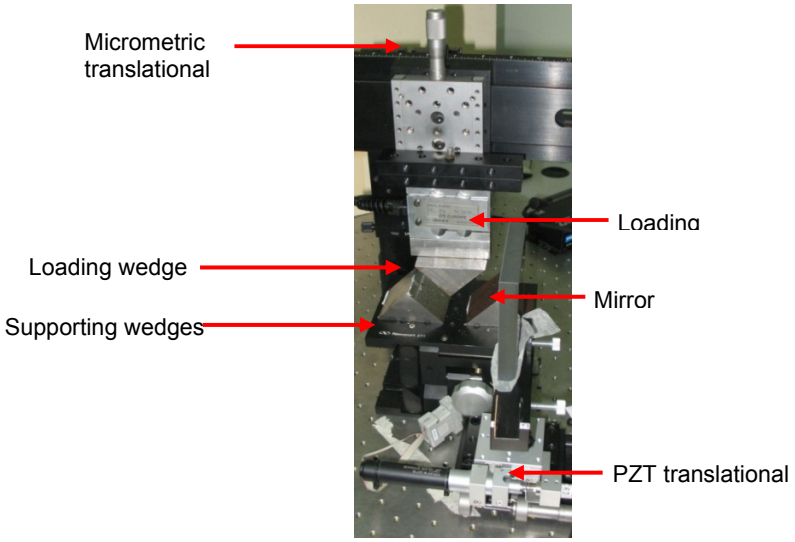

Figure 1: Loading apparatus and detail of the optical setup.

Fig. 2 shows the scheme of the optical set-up used for measuring *u*-displacements. It consists of a double illumination Lendeertz interferometer [1,2]. The light emitted by a 17 mW He-Ne laser source (λ=632.8 nm) is expanded by a 20X microscope objective lens and spatially filtered by a 10 μm aperture pin-hole. The beam emerging from the pin-hole is successively collimated by the L1 plano-convex lens (ø=2", f=40 cm). One half of the beam is then sent towards the specimen at the illumination angle θ_1= 45°. The remaining part of the beam is intercepted by the planar mirror M2 that reflects the light towards the specimen thus realizing symmetric double illumination. The mirror is placed on a piezoelectric translational stage, which allows the motion along the horizontal direction, parallel to the direction of sensitivity. The PZT is driven by a stabilized high-voltage power supply controlled by a PC. The minimum incremental displacement that can be generated is d_m=10 nm. Details of recording system are also presented in Fig. 2.

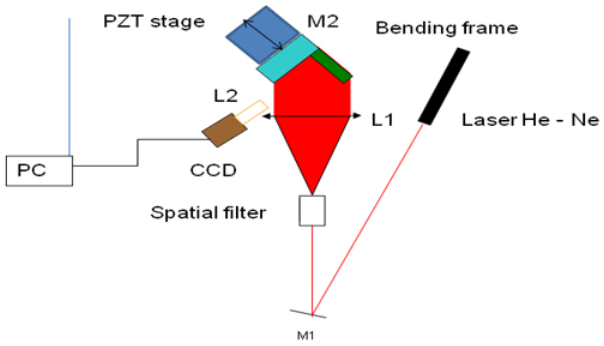

Number of pixel in the CCD sensor	1628 x 1236
Bit depth	8 bit
Field of View	21 mm
Working Distance	32 cm

Figure 2: Schematic of the double illumination ESPI setup and details of the recording system.

Each beam generates a speckle pattern on the specimen surface. The superposition of those patterns leads to have the following distribution of intensity:

$$I(x,y) = I_{01}(x,y) + I_{02}(x,y) + 2\sqrt{I_{01}(x,y)I_{02}(x,y)}\cos\gamma(x,y) \quad (1)$$

where I_{01} and I_{02} are the background intensities while γ is the phase difference between the beams.
If a point of the specimen surface displaces along the direction of sensitivity, Eq. (1) can be rewritten as:

$$I(x,y) = I_{01}(x,y) + I_{02}(x,y) + 2\sqrt{I_{01}(x,y)I_{02}(x,y)}\cos(\gamma(x,y) + \Delta\varphi(x,y)) \quad (2)$$

The phase difference $\Delta\varphi$ is related to the *u*-displacement by the following equation:

$$\Delta\varphi = \frac{4\pi}{\lambda}u\sin\vartheta \quad (3)$$

Fringes are hence iso-displacement loci and the difference in displacement between points lying on two adjacent fringes is:

$$u = \frac{\lambda}{2\sin\vartheta} \quad (4)$$

According to Eq. (4), the sensitivity of optical set-up is 447 nm.
Phase shifting was utilized in order to obtain the phase distribution of the speckle pattern. For that purpose, a shift in phase between the two beams was introduced by changing the optical path of one of the arms of the interferometer. Phase variations were produced by moving the PZT stage. Among the different phase shifting strategies available in literature [3], the five frame algorithm which consists in recording five interferograms with a relative phase shift $\delta = \pi/2$ was utilized. The intensity patterns corresponding to each phase shift can be described by the following equation:

$$I^{(n)}(x,y) = I_{01}(x,y) + I_{02}(x,y) + 2\sqrt{I_{01}(x,y)I_{02}(x,y)}\cos(\gamma(x,y) + \Delta\varphi(x,y) + n\frac{\pi}{2}) \quad (5)$$

Finally, the phase difference is computed as follows:

$$\Delta\varphi(x,y) = \tan^{-1}\left(\frac{2I^{(1)}(x,y) - I^{(4)}(x,y)}{2I^{(3)}(x,y) - I^{(5)}(x,y) - I^{(1)}(x,y)}\right) \quad (6)$$

The PZT was calibrated by recording an initial speckle pattern and moving the mirror at incremental steps of 10 nm. The speckle pattern corresponding to each shifted position was subtracted from the initial speckle pattern until a minimum of intensity was observed. The corresponding distance travelled by the PZT was related to the change of optical path yielding a 2π phase shift. Calibration of the camera pixel was done by recording the image of a calibration target and sampling the distance between two calibration marks with a certain number of pixels. The spatial calibration was 15 µm.
In the processing phase for each shift of phase the difference between the recorded image and the reference image was determined by digitally subtracting speckle patterns. A 9x9 pixel square median filter was then applied to the five images in order to reduce noise. A mask was applied in order to select the region of interest. Eq. (5) was used in order to obtain the wrapped phase. Phase unwrapping operation was carried out by means of the minimum spanning tree algorithm [4]. Finally, displacement maps were recovered by using the scaling Eq. (3).

FEM ANALYSIS

A finite element model, with real sizes of the specimens tested, was developed in order to simulate the 3-point-bending test. Because of structural symmetry, only one half was modeled. The region of interest considered along the x-direction was about 63 mm. Kinematic constraints were imposed in order to obtain a symmetric model and to correctly reproduce the mechanism for loading. FE analysis was carried out with the ANSYS® 10.0 commercial software [5]. The specimen was modeled with three-dimensional elements SOLID45 including 8 nodes each of which has 3 degrees of freedom, the translations in the coordinate directions X, Y and Z. Although specimens' thickness is small compared to length, the specimen under 3-point-bending was however modeled as a 3D specimen in order to account for asymmetries eventually occurring in the loading process or related with constraint conditions.

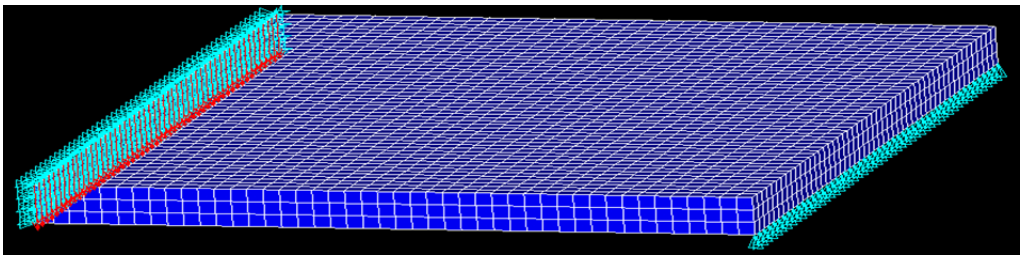

Figure 3: Finite element model of the 3-point-bending test numerically simulated.

The specimen materials were assumed as isotropic and linearly elastic. This assumption obviously correct for the titanium specimen should also be justified for the sintered one by the fact that SLM specimens are realized by random strategy on each layer, so each layer could be considered as isotropic. The experimental evidence seems to confirm this assumption: in fact, the u_x displacement measured through the thickness became null at the specimen midplane.
Convergence analysis was carried out in order to refine the model and to obtain a mesh independent solution. The mesh included 53328 elements and 63546 nodes for the titanium specimen and 36432 elements and 43610 nodes for the sintered component. (Fig. 3 with indications of loads and constraints is representative of both materials). Mesh size was consistent with sampling of the speckle pattern. All finite element analyses were run on a standard PC equipped by an Intel® Pentium Dual-Core processor and 3GB RAM memory. The structural analysis was completed in about 5 minutes.

RESULTS AND DISCUSSION

The horizontal displacement measured by ESPI was taken as target value of FE analysis. In both cases, for titanium and SLM specimens, the area monitored during experimental test was located 500 nm far from the constraint wedge and far enough from the region where the load is applied, in order to avoid the influence of local phenomena. Moreover, in this area the displacement values were symmetric with respect to the neutral plane. Young's modulus of Ti6Al4V used in the numerical model was 110 GPa [6] and Poisson's ratio was fixed to 0.32. The optimization minimizes the gap between displacement measured by ESPI (**Δu_x Exp)** and those evaluated by FEM analysis (**Δu_x FEM**). Tab. 2 summarizes results related to the optimization process: it can be observed that the error on measured displacements decreases as the loading level increases (it seems that rigid body motions affect experimental measurements and reduce at higher loads) and that the residual error on displacements is less than 1%. Mechanical properties calculated for titanium alloy by means of the proposed hybrid procedure were obtained. The study of SLM specimen started from Young's modulus of 166 GPa [7] related to specimens built with very similar process parameters of the SLM parts studied in this work. After FEM model validation for titanium specimen, SLM component was analyzed by the same code changing geometrical dimensions and starting mechanical properties. Tab. 3 shows experimental and FEM results for SLM specimen. Also in this case the proposed methodology seems to work: the error on measured displacements decreases as the loading level increases and that the residual error on displacements is less than 8%. Mechanical properties calculated for SLM specimen are: Young's modulus 140 GPa and 0,3 Poisson coefficient. The non perfect isotropy of SLM material (as supposed in building FE model) could be a reasonable explanation of the slight and rather constant error of about 8% between experimental and numerical values.

As expected, iso *u*-displacement bands are almost parallel in the specimen region near the supporting wedges. The experimental pattern (Fig. 4) is in excellent agreement with FE results (Fig. 5). The difference in displacement between points located on vertical lines at different distances from the constrained edge of the specimen was found to be insensitive to the position. The same conclusion can be drawn for all load levels considered in the experiments.
Remarkably, the experimentally measured values of *u*-displacement were found to be symmetric with respect to the midplane of the specimen. This seems to confirm the assumption of isotropy of SLM material made in the numerical analysis.

Load [g]	Δu_x Exp [nm]	Δu_x FEM [nm]	Exp fit [nm]	Error %
304	278	334	313.45	-6.2
467	455	513	499.05	-2.7
69	758	735	729.07	-0.8
870	1058	956	957.95	0.2
1072	1116	1177	1187.97	0.9

Table 2: Percentage displacements' difference on titanium specimen

Load [g]	Δu_x Exp [nm]	Δu_x FEM [nm]	Exp fit [nm]	Error %
130	224	200	221.29	10.6
293	464	450	489.78	8.8
330	520	508	550.73	8.4
504	890	776	837.34	7.9
529	919	814	878.52	7.9
695	1188	1069	1151.95	7.7
706	1118	1087	1170.07	7.6
810	1318	1246	1341.38	7.6

Table 3: Percentage displacements' difference on sintered specimen

CONCLUSION

This paper presents an hybrid approach to characterize new materials or materials realized by means of non-conventional techniques. Titanium Ti6Al4V and SLM specimens were considered in order to define the experimental set up and to validate the numerical model that should be used to obtain mechanical properties of materials.

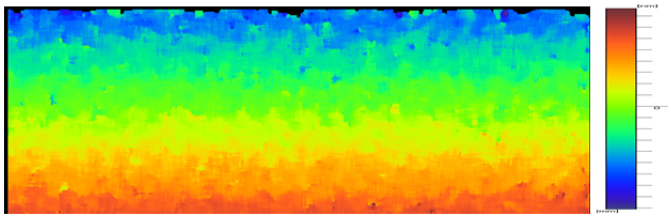

Figure 4: Horizontal displacement map near supporting wedge of the sintered material.

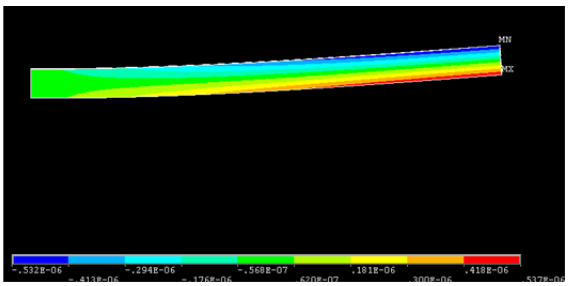

Figure 5: Horizontal displacement map evaluated via FEM of the sintered material

REFERENCES

[1] G.L. Cloud, Optical Methods in Engineering Analysis, Cambridge University Press, New York (USA), (1998).
[2] C. Sciammarella, Exp. Mechanics, 43(1) (2006) 1.
[3] K. Creath, Applied Optics, 24(18) (1995) 3053.
[4] N. H. Ching, D. Rosenfeld, M. Braun, IEEE Transactions on Image Processing, 1(3) (1992) 355.
[5] The ANSYS 10.0 Users' Manual, Swanson Analysis System Inc., (2005).
[6] C. Casavola, C. Pappalettere, F. Tattoli, Mechanics of Materials, 41(3) (2008) 231.
[7] C. Casavola, S. L. Campanelli, C. Pappalettere, Journal of Strain Analysis, 44(1) (2009) 93.